Express Polymer Letters Vol.17, No.5 (2023) 512–526
Available online at www.expresspolymlett.com
https://doi.org/10.3144/expresspolymlett.2023.38

Research article

Construction of topological entanglement at the interface between silicone rubber and nano-silica to achieve excellent crack extension resistance

Linru Jiang[1], *Jingchao Li*[1,3], *Weizhen Zhang*[1], *Yonglai Lu*[1,2*], *Liqun Zhang*[1,2]

[1]State Key Laboratory of Organic-Inorganic Composites, Beijing University of Chemical Technology, 100029 Beijing, China
[2]Engineering Research Center of Elastomer Materials Energy Conservation and Resources, Ministry of Education, Beijing University of Chemical Technology, 100029 Beijing, China
[3]Beijing Key Laboratory of Wood Science and Engineering & MOE Key Laboratory of Wooden Material Science and Application, Beijing Forestry University, 100083 Beijing, China

Received 18 October 2022; accepted in revised form 12 December 2022

Abstract. The poor tear resistance of silicone rubber dramatically limits its application range. In this study, a topological entanglement structure of molecular chains was constructed at the interface between the matrix and silica by introducing epoxidized silicone rubber into silicone rubber/silica composites. We found that this topologically entangled structure could improve the crack propagation resistance of the composites by inducing the orientation of molecular chains. The results showed that adding 5 phr of 15% epoxy silicone rubber raised the silicone rubber composite's tear strength and elongation at break, they increased by 330% and 140%, respectively. This work provides a new idea for preparing silicone rubber composites with high tear resistance to better expand the application field of silicone rubber.

Keywords: *rubber, polymer composites, mechanical properties, topological entanglement, epoxidized silicone rubber*

1. Introduction

The special Si–O bond structure in silicone rubber gives it a variety of excellent properties, such as excellent thermal stability, aging resistance, and biocompatibility. These excellent characteristics make it play an irreplaceable role in aerospace, medical instrument industry, construction, electronics industry, chemical industry and transportation, and other fields [1–10]. Carbon nanoparticles were added to silicone rubber to increase its mechanical and electrical characteristics to be utilized in strain sensors [11–14]. Silicone rubber with thermochromic phase change microcapsules has thermochromic properties and recyclability and can be used in the field of security labels and temperature sensors [15]. Due to its high resistance to extreme temperatures and stable chemical properties, silicone rubber may be utilized as a thermal insulation material in the aerospace field [16, 17]. The application of phenyl silicone rubber in aerospace is made available by its radiation resistance and dampening properties [18, 19]. Fuel delivery systems in automobiles and aerospace employ fluorosilicone rubber that is resistant to fuel and heat [20–22]. In the shipping sector, silicone rubber has been utilized in ecological fouling prevention coating [23–25]. However, the poor mechanical properties and low tear strength of silicone rubber compared to other rubbers have greatly limited the application range of silicone rubber [26, 27]. Therefore, there is an urgent need for effective strategies to improve their mechanical

---

[*]Corresponding author, e-mail: luyonglai@mail.buct.edu.cn

properties and crack resistance significantly. To improve the mechanical properties of silicone rubber, researchers have improved the tear resistance of silicone rubber by adding reinforcing agents, cross-linking agents, improving branched groups of silicone rubber, and blending with other rubbers [28–32]. Silica is a very effective and widely used reinforcing agent for silicone rubber due to the interfacial contact between silica and silicone rubber, which improves the mechanical properties of silicone rubber [33–39]. Therefore, the poor tear resistance of silicone rubber may be enhanced by improving the interfacial contact between silica particles and silicone rubber. Fang *et al*. [40] prepared superhydrophobic nano silica, which improved the mechanical properties of silicone rubber composites, especially the elongation at break. Yan *et al*. [41] modified nano-silica by surface modifiers hexamethyldisilazane (HMDS) and methacryl-functional silane (KH570), and adjusted the modification dosage to regulate the mechanical properties of silicone rubber, especially the tear resistance. Park *et al*. [42] added a vinyl silane coupling agent to nano-silica to modify it. Modified nano-silica was added, increasing the liquid silicone rubber's tensile strength by 27.9 times. Xu *et al*. [43] found that the tear strength of silicone rubber blended with different vinyl content was higher than that of single vinyl silicone rubber, with a maximum tear strength of 31.55 kN/m. Chen *et al*. [44] co-cross-linked silicone rubber with different vinyl contents. A nonuniform network is formed in nano-silica reinforced silicone rubber to enhance mechanical properties, among which the tear strength reached 41 kN/m. Sarath *et al*. [45] added 7 phr of exfoliated graphite (EG) to the silicone rubber to promote uniform stress transfer in the silicone rubber, and the tear strength was increased from 20 to 30 kN/m. Cao *et al*. [46] added 2 phr of high vinyl silicone oil (HVSO) to form a special cross-linked network structure, resulting in an 18.5% increase in the tear performance of the composite. Wang *et al*. [47] obtained thermoplastic vulcanizates (TPVs) by blending vinylidene fluoride, fluoroelastomer, and silicone rubber and adding a certain amount of vulcanizing agent to vulcanize them. It was also found that the good interfacial compatibility of vinylidene fluoride and fluoroelastomer could improve the mechanical properties of TPVs with a tear strength of 58 kN/m. Dong *et al*. [48] synthesized γ-chloropropyl polysiloxane and added vulcanizing agents with polyamino polydimethylsiloxane end groups to form a concentrated cross-linked network in silicone rubber. The tear strength reached a maximum of 45.5 kN/m when the [N–H]/[$(CH)_3Cl$] ratio was 1. However, these conventional methods of toughening have drawbacks of their own. For instance, while increasing its hardness, silicone rubber's great qualities, such as its ability to withstand both high and low temperatures and its resistance to aging, were diminished. Additionally, the production of modified nano-fillers is a costly and challenging operation. Because dense cross-linking stiffens the rubber, strengthening the chemically cross-linked network of silicone rubber and introducing a non-homogeneous network would minimize its own elongation at break while improving tear strength. Kim *et al*. [49] prepared highly entangled polymers with a fabric-like topology that resolved the conflict between stiffness and toughness and achieved both high toughness and low hysteresis. Liu *et al*. [50] prepared topoarchitected polymer network (TPN) hydrogels in which each block had a polymer network consisting of dense cross-links, and the matrix had a sparsely cross-linked polymer network. The polymer networks of the block and matrix were firmly adhered together by topological entanglement. At the crack tip of the TPN, the enormous strain in the soft matrix spreads high stress over the length of the rigid block, making the TPN more challenging. Gao *et al*. [51] have successfully prepared an ideal mechanically interlocked composite structure by coarse particle molecular dynamics simulations. The structure permits the matrix chains to cross the rings formed by the end-functionalized chains that have been grafted to the surface of the nanoparticles, improving the tensile stress of the system significantly up to 700%

In this paper, high vinyl silicone rubber (HMVQ) was prepared by anionic polymerization. To produce epoxidized silicone rubber (EMVQ), epoxy groups were introduced to the silicone rubber's molecular chain after the vinyl in the chain was reacted with 3-chloroperbenzoic acid. Silicone rubber with high tear resistance was prepared by adding EMVQ, ordinary silicone rubber (110-2), and fumed silica. The epoxy group would interact with the hydroxyl group of silica to form covalent bonds [52, 53]. EMVQ's molecule chains create polycyclic structures on the silica that can be topologically entangled with the matrix silicone rubber molecular chains. It is found that the topological entanglement can effectively inhibit crack propagation by inducing the orientation of molecular chains, resulting in a composite with excellent tear strength. This method avoids the drawback that chemical cross-linking cannot bestow the ability to transfer molecular chains in the network structure, as opposed to conventional toughening methods. More molecular chains can bear stress through topological entanglement. The elongation at break of silicone rubber was also enhanced, in addition to the tear resistance, without weakening other properties. In this paper, an effective method to improve the crack propagation resistance of silicone rubber composites was demonstrated. It is important for the expansion of the application of silicone rubber. In addition, the influence mechanism of topological entanglement of molecular chains at the interface between silicone rubber and nano-filler on the tearing performance of the composites was expounded.

2. Materials and methods

2.1. Materials

Methyl vinyl silicon rubber (MVQ) with vinyl content of 0.17% was purchased from Dongjue Organosilicon (110-2, Tianjin, China); octamethyl cyclotetrasiloxane (D_4, 99%, Shandong, China), tetramethyl tetravinyl cyclotetrasiloxane (V_4, 98%, Shandong, China) decamethyltetrasiloxane, methanol, and catalyst alkali glue (2%, Shandong, China) were obtained from Shandong Dongyue Organosilicon Materials Co., Ltd.; 3-chloroperbenzoic acid (MCPBA) was purchased from Shanghai Macklin Biochemical Co., Ltd. (85%, Sanghai, China); 2,5-dimethyl-2,5-di(tert-butylperoxy)hexane (DBPH) was purchased from Shangyu Shaofeng Chemical Co., Ltd (92%, Zhejiang, China). Chlorobenzene was purchased from the Beijing Ruixiang Nengyuan Trading Co., Ltd (≥99%, Beijing, China). Silica was purchased from Degussa (A200, Frankfurt, Germany).

2.2. Synthesis of HMVQ and EMVQ

The mechanism of synthesis is the anion ring-opening reaction of monomer D_4 and V_4 catalyzed by catalyst alkali glue; the reaction process is shown in Figure 1a.

Different amounts of D_4 and V_4 were added to the three-necked flask, as shown in Table 1. The stirring rate was maintained at 150 rpm and the temperature was increased to 80 °C. Turn on the vacuum pump and reduce the vacuum degree to approximately –0.09 MPa. Raw materials are dehydrated for 1 h. The vacuum pump was turned off to return the system to normal pressure. The system was added with catalyst alkali gel and blocking agent, and then warmed up to 113 °C under nitrogen protection for 3 h. Then the temperature is raised to 163 °C and the catalyst alkali gel decomposes trimethylamine. Finally, trimethylamine and unreacted monomers are removed under a vacuum. Since the viscosity of the system will gradually increase during the reaction, we need to continuously adjust the rate of magnetic stirring to ensure the homogeneity and stability of the system during the reaction.

Table 1. Experimental formulation of HMVQ with different vinyl content.

Raw materials	**V_c [%]**		
D_4	90	85	80
V_4	10	15	20
DMTS	0.06	0.06	0.06
Catalyst alkali glue	0.015	0.015	0.015

HMVQ and chlorobenzene were added to a three-necked flask and dissolved with stirring at 55 °C. Then, the MCPBA was added to the system. The temperature of the system was maintained at 55 °C for 40 h. The reaction is depicted in Figure 1b. In order to precipitate out the organic acid, the temperature of the system is maintained at -20 °C for 12 h. Then, the organic acid is filtered by the screen. Methanol is added to the system, and then a white precipitate appears. It is dried in a vacuum oven.

2.3. Preparation of composites

MVQ and EMVQ were added to the open mill (Table 2). Then 40 phr of silica were added to the

Table 2. The formulation of compounds.

Samples	**Weight of different gums**		**DBPH [phr]**	**Silica [phr]**
	110-2 [phr]	**EMVQ [phr]**		
MVQ	100.0	0	0.08	40
EMVQ10-2.5	97.5	2.5	0.08	40
EMVQ10-5	95.0	5.0	0.08	40
EMVQ10-7.5	92.5	7.5	0.08	40
EMVQ10-10	90.0	10.0	0.08	40
EMVQ15-2.5	97.5	2.5	0.08	40
EMVQ15-5	95.0	5.0	0.08	40
EMVQ 5-7.5	92.5	7.5	0.08	40
EMVQ15-10	90.0	10.0	0.08	40
EMVQ20-2.5	97.5	2.5	0.08	40
EMVQ20-5	95.0	5.0	0.08	40
EMVQ20-7.5	92.5	7.5	0.08	40
EMVQ20-10	90.0	10.0	0.08	40

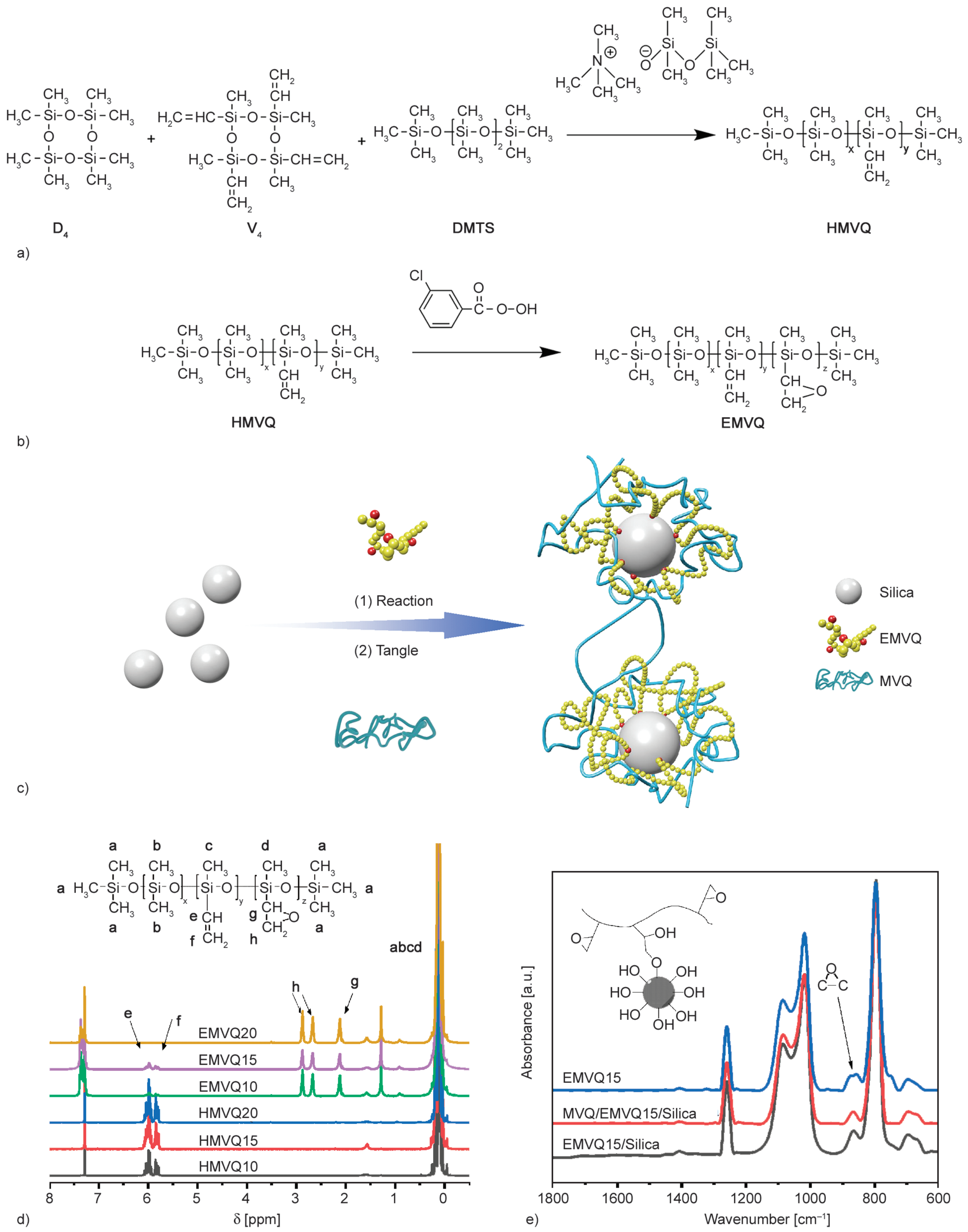

Figure 1. a) The synthesis of HMVQ; b) the synthesis route of EMVQ; c) ^{1}H NMR spectra of MVQ and EMVQ; d) topological entanglement allows the MVQ's molecular chain to cling to the filler; e) infrared spectra of EMVQ15 with compounding rubber.

open mill. The blend was placed at room temperature for 24 h. The blend was tested by a moving die rheometer (MD-3000A, Gotech Testing Machines Inc, Taiwan, China) to get the positive vulcanization time t_{90} at 170 °C. The blend was molded at 10 MPa for the positive vulcanization time t_{90} in a plate vulcanizing machine (XQLB-350×350, Gotech Testing Machines Inc, Taiwan, China) to obtain vulcanized silicone rubber sheet (120 mm × 120 mm × 1 mm).

2.4. Characterization

2.4.1. Structural characterization

The samples were measured using gel permeation chromatography (GPC Waters 1515, Waters, USA). Dissolving the samples in tetrahydrofuran (THF) at a concentration of 2–4 mg/ml. After the samples were completely dissolved and filtered, then tested to obtain molecular weight and molecular weight distribution. The samples were tested by Fourier transform infrared spectrometer (Tensor 27, Bruker, USA) to obtain infrared absorption spectra in the range of 600–4000 cm^{-1}.

The samples were dissolved in deuterated chloroform. The samples were subjected to proton nuclear magnetic resonance (^{1}H NMR) spectroscopy using a nuclear magnetic resonance spectrometer (AV400, Bruker, USA).

The orientation of the uniaxially stretched sample can be described by Equation (1). In the formula α is the angle between the leap moment and the axis of the molecular chain. Thus, $(R-1)/(R+2)$ is used to describe the orientation of the molecular chain. Absorbances of the investigated absorption band in the perpendicular and parallel directions are recorded as $A_\perp$ and $A_{//}$, respectively, and the infrared dichroism ratio is $R = A_{//}/A_\perp$. Polarization modulation experiment performed by Fourier transform infrared spectrometer with a polarization filter. The sample is fixed to a device that can be adjusted for different tensile strains in Fourier transform infrared spectrometer:

$$f = \frac{R-1}{R+2}\cdot\frac{2}{3\cos^2\alpha - 1} \tag{1}$$

2.4.2. Physical and mechanical performance

According to GB/T528-2009 and GB/T 529-2008 standards, tensile strength and tear strength are tested using Servo Control System Universal Testing Machine (AI-7000-SU1, Gotech Testing Machines Inc, Taiwan, China). The hardness is measured by Shore A hardness tester (SAC-J, Beijing Ruida Yuchen Instrument Co., Ltd, Beijing, China) according to GB/T531-2008 standard. The samples were tested by LF-NMR (VTMR20-010V-I, Niumag, ShangHai, China) to obtain cross-linking density.

2.4.3. Microscopic characterization

In order to obtain the morphology of the stretched sample, the sample needs to be stretched to a predetermined strain, fixed and then polished. The morphology of the samples was obtained by atomic force microscope (Multimode8, Bruker, USA). At a scan rate of 1 Hz, images with an area of 5×5 μm were captured at a resolution of 256×256 pixels. The morphology of vulcanized silicone rubber was seen using a scanning electron microscope (S-4800, Hitachi, Japan). Samples were created using the low-temperature brittle fracture method, and the surface was then gold-sprayed before the morphology at the samples' fractures was observed. Vulcanized silicone rubber is characterized by a transmission electron microscope (H-9500, Hitachi, Japan).

2.4.4. Rubber process analysis (RPA)

The Payne effect of the blend was analyzed by an RPA2000 rubber process analyzer (Alpha Technologies, USA) at 60 °C, frequency of 1 Hz, and a strain range of 0.3 to 100%.

3. Results and discussion

3.1. Construction and microstructural characterization of composite materials

3.1.1. Structural characterization of EMVQ

As observed in Figure 1d, the peaks in the ^{1}H NMR spectrum at chemical shift 0 ppm are hydrogen on methyl in polysiloxane, while the peaks at chemical shifts 5.98 and 5.83 ppm are hydrogen in vinyl [54, 55]. Chemical shifts of 2.88, 2.66, and 2.11 ppm served as evidence of the conversion of vinyl to epoxy group [56, 57]. The ^{1}H NMR spectrum's peaks were integrated, and the epoxy group content (e) and the vinyl content (v_i) were determined using Equations (2) and (3), respectively (3):

$$e = \frac{E}{\frac{M-V-E}{2}+E+V}\cdot 100\% = \frac{2E}{E+V+M}\cdot 100\% \tag{2}$$

$$v_i = \frac{V}{\frac{M-V-E}{2}+E+V}\cdot 100\% = \frac{2V}{E+V+M}\cdot 100\% \tag{3}$$

where V is the area of the hydrogen peak of the vinyl group in the ^{1}H NMR spectrum. M is the area of the hydrogen peak of the methyl group in the ^{1}H NMR

Table 3. Content of each component in HMVQ and EMVQ.

Samples	Vinyl content [%]	Epoxy group content [%]	M_n [10^4 g/mol]	M_w [10^4 g/mol]	PDI
HMVQ10	11.3	–	40.94	88.67	2.16
HMVQ15	19.2	–	27.16	68.91	2.54
HMVQ20	27.1	–	23.19	79.78	3.44
EMVQ10	1.31	9.80	26.25	69.30	2.64
EMVQ15	3.21	13.56	22.00	56.78	2.58
EMVQ20	0.11	18.80	13.86	44.12	3.18

spectrum and E is the area of the hydrogen peak of the epoxy group in the ^{1}H NMR spectrum.

In comparison to HMVQ, EMVQ's relative molecular weight altered more, and the polydispersity index (PDI) rose marginally (Table 3). The system's high concentrations of 3-chloroperbenzoic acid and benzoic acid may have caused the molecular weight to drop due to the breakdown of the molecular chain and the ring-opening side reaction of the epoxy group.

3.1.2. Infrared spectroscopic analysis of the compound of EMVQ15

As shown in Figure 1e, the epoxy group's characteristic peak is at 882 cm^{-1}, the Si–O–Si stretching vibration's absorption peak is at 1089 cm^{-1}, and the peak at 800 cm^{-1} is attributable to the Si–C stretching vibration [58]. The distinctive peak of the epoxy group at 882 cm^{-1} of the EMVQ15/Silica blend has vanished when compared to the EMVQ15 and EMVQ15/Silica blends (Figure 1e). This indicates that the epoxy group has reacted with the hydroxyl group and the polycyclic structure has been formed on the silica surface. We create the architecture of topological entanglement (Figure 1c).

3.1.3. Scanning electron microscopy (SEM) and transmission electron microscopy (TEM)

In Figure 2a$_1$, the cross-sectional morphology of MVQ fracture was rough, with fewer and comparatively concentrated white highlights. In comparison to MVQ, the shape of the fracture cross-section was flatter in Figure 2a$_2$, and the silica dispersion was better. Silica was less agglomerated in Figure 2a$_3$ and Figure 2a$_4$. It is easy to find the parabolic structure of the fracture cross-section in Figure 2a$_4$, which denotes a significant concentration of stress during the stretching process. In Figure 2a$_5$, It is difficult to see the rough surface shape.

Agglomeration of fillers means poor dispersion of silica in Figure 2b$_1$. The silica showed evenly dispersed, and no evident agglomeration was observed in Figure 2b$_2$–2b$_5$.

In conclusion, the dispersion of silica in MVQ was improved by the addition of EMVQ and becomes better as the amount of EMVQ rises.

3.2. Curing and mechanical properties of materials

3.2.1. Vulcanization characteristic curve

The vulcanization characteristics of EMVQ15 with different dosages were shown in Table 4 and Figure 3a. As the EMVQ amount was increased, the minimum torque (M_L) and the maximum torque (M_H)were reduced. $M_H - M_L$ reflects the influence of filler on rubber reinforcement. But $M_H - M_L$ showed a trend of first decreasing and then increasing, and silica was distributed more uniformly. This was because silica reacted with epoxidized silicone rubber to form covalent bonds, which caused better dispersion of silica

Table 4. Vulcanization characteristics of different formulated composites.

Samples	M_L [dN·m]	M_H [dN·m]	$M_H - M_L$ [dN·m]	Scorch time, t_{10} [min]	Cure time, t_{90} [min]
MVQ	13.12	23.74	10.62	2.14	8.24
EMVQ10-2.5	13.46	22.89	9.43	1.55	8.05
EMVQ10-5	12.53	23.44	10.91	2.09	9.25
EMVQ10-7.5	10.11	21.89	11.78	2.01	12.54
EMVQ10-10	9.27	22.33	13.06	2.02	10.28
EMVQ15-2.5	13.45	23.07	9.62	2.10	12.34
EMVQ15-5	11.38	21.63	10.25	1.97	9.49
EMVQ15-7.5	9.52	20.89	11.37	1.78	11.32
EMVQ15-10	9.21	20.58	11.37	1.68	13.28
EMVQ20-2.5	10.17	19.08	8.91	0.29	7.19
EMVQ20-5	8.39	16.53	8.14	0.29	6.27
EMVQ20-7.5	6.28	16.16	9.88	1.53	7.40
EMVQ20-10	6.26	17.26	11.00	1.56	8.36

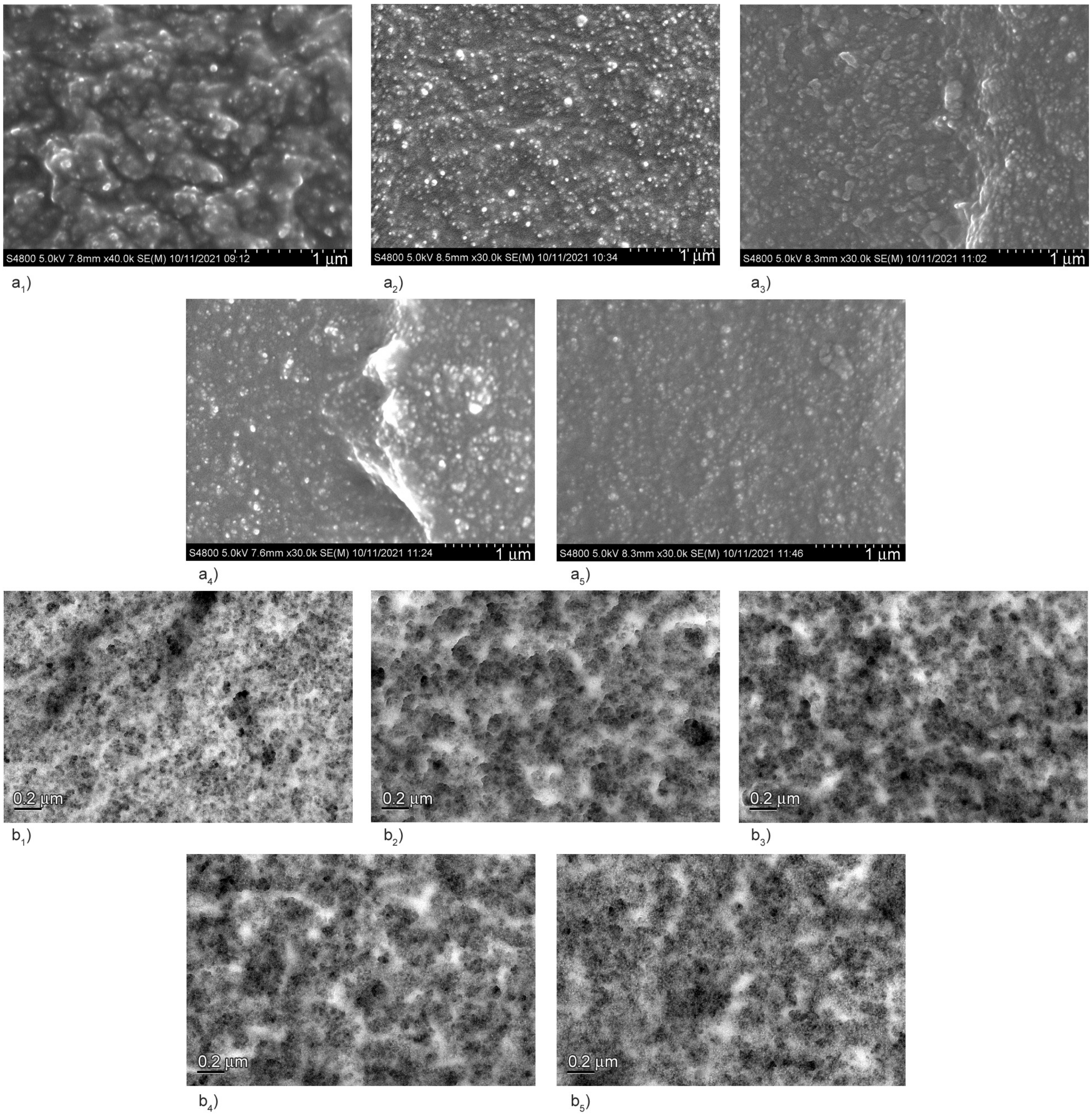

Figure 2. a) The SEM of composite materials: a_1) MVQ, a_2) EMVQ-15-2.5, a_3) EMVQ15-5, a_4) EMVQ15-7.5, a_5) EMVQ15-10; b) the TEM of composite materials: b_1) MVQ, b_2) EMVQ-15-2.5, b_3) EMVQ15-5, b_4) EMVQ15-7.5, b_5) EMVQ15-10.

[59, 60]. The scorch time t_{10} was also steadily reduced. The positive vulcanization time t_{90} ranged from 8 to 13 min. M_L and M_H were reduced, but $M_H - M_L$ showed a trend of first decreasing and then increasing.

3.2.2. RPA

The storage modulus (G')-strain curves of EMVQ15 with different dosages are shown in Figure 3b. The filler network is strong due to the agglomeration of the filler at low strain. The storage modulus (G') is also high. The Payne effect refers to the phenomenon wherein G' dramatically drops with increasing strain. The higher initial G' indicated the poor dispersion of silica. As the amount of EMVQ15 was increased, the initial energy storage modulus gradually declined. The weakening of the Payne effect was indicated by this trend. Thus, silica is better dispersed in the matrix silicone rubber.

3.2.3. Mechanical properties

The mechanical properties of EMVQ with different dosages are shown in Table 5. The tear strength of composites was not improved by the addition of

Table 5. Mechanical properties of different formulations.

Samples/ Performance	Tensile strength [MPa]	Stress at 100% [MPa]	Stress at 300% [MPa]	Elongation at break [%]	Shore A hardness	Tear strength [kN/m]	Cross-link density [10^{-4} mol/ml]
MVQ	9.6±0.5	1.9±0.1	7.5±0.5	357±25	61±1	19±1	0.8797±0.0122
EMVQ10-2.5	10.6±0.9	1.4±0.1	5.4±0.4	404±37	61±2	20±1	1.1226±0.0162
EMVQ10-5	10.7±0.7	1.4±0.1	4.4±0.2	517±20	60±2	20±3	0.8953±0.0064
EMVQ10-7.5	10.4±0.6	1.3±0.1	3.7±0.5	557±45	59±1	21±1	0.8777±0.0065
EMVQ10-10	10.0±0.4	1.3±0.1	3.7±0.1	567±26	57±2	24±2	0.8890±0.0052
EMVQ15-2.5	10.5±0.8	1.4±0.1	6.5±0.2	404±22	55±1	19±1	0.9033±0.0035
EMVQ15-5	11.3±0.9	1.3±0.1	5.1±0.3	510±28	54±2	57±6	0.9277±0.0117
EMVQ15-7.5	10.7±0.5	1.1±0.1	3.5±0.3	576±48	52±1	52±5	0.8987±0.0086
EMVQ15-10	9.5±0.5	1.1±0.1	2.8±0.2	619±34	52±2	40±5	0.8659±0.0055
EMVQ20-2.5	10.7±0.6	1.1±0.1	7.5±0.3	459±43	53±2	15±1	0.9280±0.0106
EMVQ20-5	10.7±0.4	0.9±0.1	5.0±0.5	580±25	53±1	54±5	0.9387±0.0291
EMVQ20-7.5	10.3±0.4	0.8±0.1	4.8±0.2	602±39	53±1	37±4	0.9340±0.0149
EMVQ20-10	9.6±0.8	0.9±0.1	3.2±0.5	632±14	56±1	22±5	0.8280±0.0140

EMVQ10. The tear strength of composites with the 5 phr of EMVQ15 could reach 57 kN/m, which was three times the tear strength of the MVQ. The tear strength of composites significantly increased after the addition of EMVQ15. The tear strength of the composites with EMVQ20 was enhanced but not as

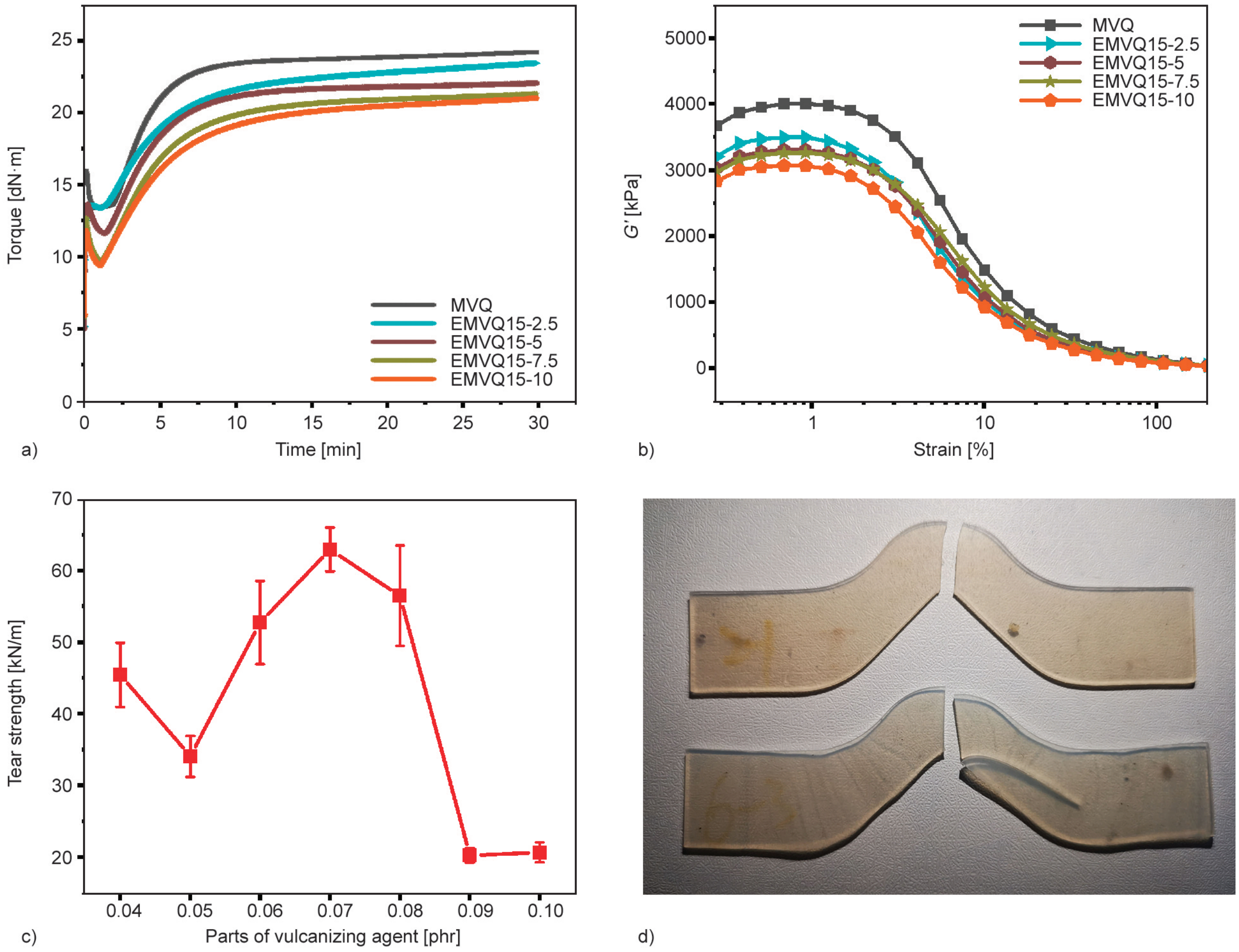

Figure 3. a) Vulcanization curves of EMVQ15 and MVQ; b) relationship between energy storage modulus and strain of EMVQ and MVVQ; c) tear strength of EMVQ15-5 after adding different amount of vulcanizing agent; d) photograph of EMVQ and MVQ after tearing fracture.

good as EMVQ15. When the EMVQ's epoxy group content was certain, we can observe a similar trend for composites with high tear resistance. As the EMVQ amount was increased, the tear strength first remained constant, then increased, and final falls. There was a tendency for the crosslink density to rise and then fall as the number of EMVQ increased. This was because the structure of the molecular chain network of the system would be influenced by the number of topological entanglements reaching a specific threshold. When there were too many rings, the number of silicone rubber molecular chains in each ring was relatively reduced. Only sliding, not tangling, occurred between molecular chains in the ring. This was why the elongation at break consistently increased as the amount of EMVQ increased.

The tear resistance of silicone rubber cannot effectively be improved when the added EMVQ's degree of epoxidation is low. The excess EMVQ's degree of epoxidation may be detrimental to silicone rubber's tear resistance. Topological entanglement between the molecular chains of the matrix rubber and silica was impacted by polycyclic structures determined by the degree of epoxidation of EMVQ of different sizes. The MVQ's molecular chains can slide around the ring easily when the ring structure was too big. Again, the number of rings was relatively increased when the ring structure is too small. Neither of them can form effective topological entanglement. This was why the elongation at break was consistently increased as the epoxy group content of EMVQ increased.

Since topological entanglement under stress may spontaneously adjust the movement of the matrix rubber's molecular chains, composites' stress at 300 percent of strain dropped as EMVQ dosage increased.

We obtained the fracture energy and tear energy by integrating the area of the stress-strain curve. Compared to MVQ, the tensile strength of EMVQ15 did not increase, and the tensile fracture energy of EMVQ15 increased 160% (Figures 4a and 4b). In contrast, the tearing energy of EMVQ15 increased 1570% in Figure 4c. The tear strength and tensile strength of MVQ15-2.5 were not improved. However, the fracture energy and strain of EMVQ15-2.5

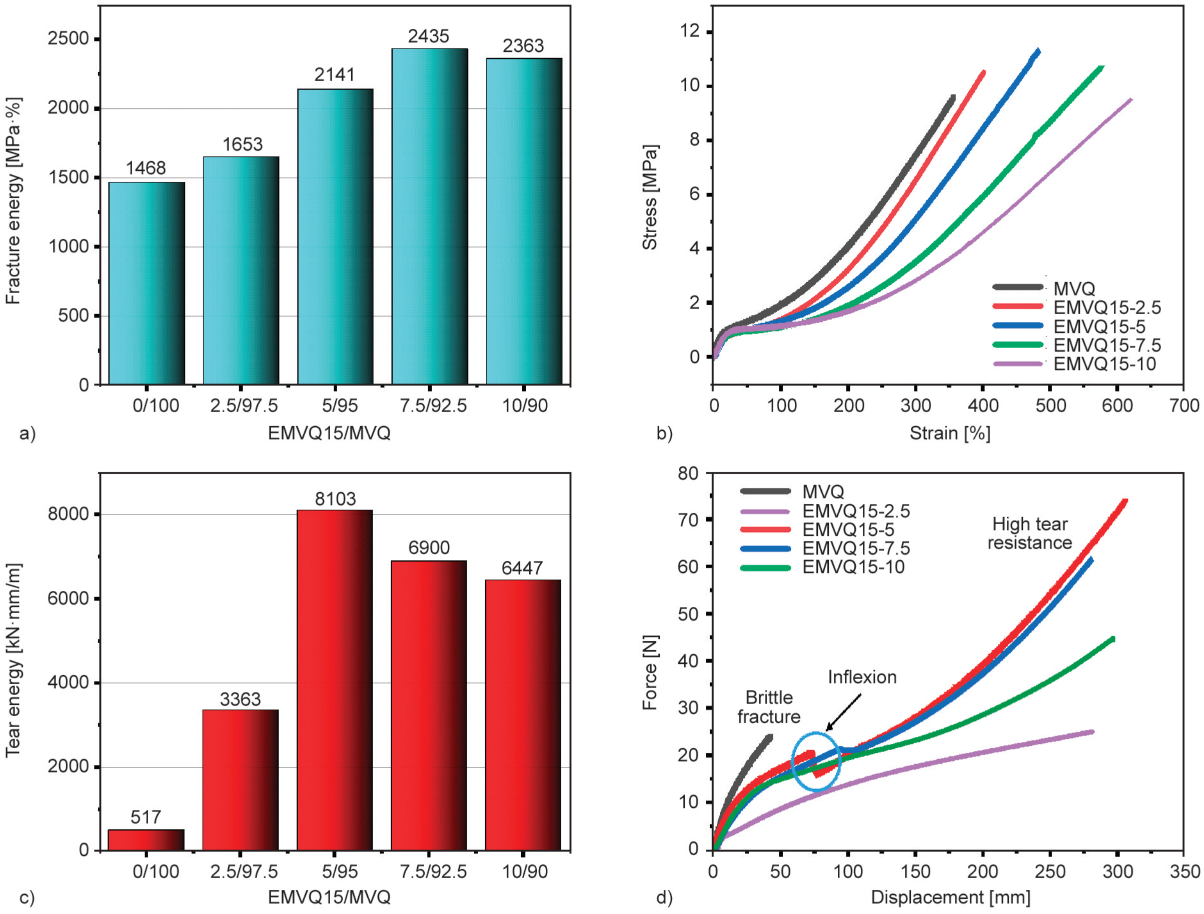

Figure 4. a) Histogram of fracture energy; b) histogram of tearing energy; c) stress–strain curves; d) tear force–elongation curves.

was raised. Samples with high tear strength displayed unusual forks along the fracture routes (Figure 3d). Samples with high tear strength displayed inflections on the curves (Figure 4d). This was because the molecular chain of the matrix rubber slid in the polycyclic structure, allowing the molecular chain to orient in the stretching direction, thus forcing the tear to deflect the original path.

The movement of molecular chains is affected by chemical cross-linking networks. Thus, there will be an appropriate crosslinking network [61]. The tear strength reaches 63 kN/m at 0.07 phr of vulcanizing agent (Figure 3c). After the amount of vulcanizing agent exceeds 0.08 phr, the tear strength is not increased.

3.3. Analysis of the principle

To obtain insight into how topological entanglement improves the toughness of silicone rubber, AFM experiments were performed on composites with different EMVQ dosages. We can see how the microstructure of EMVQ15-5 changed during the uniaxial stretching operation (Figure 5a). Darker areas denote lower modulus, and brighter areas denote higher modulus. The overall brightness of the sample is low in the absence of strain, indicating that the modulus is quite low in Figure 5a_1. The spots with high brightness have become more and more when the strain of the sample was 100% in Figure 5a_2. When the strain was raised by 300%, Figure 5a_3 showed a high-brightness fiber structure in the stretching direction. This was because the stress caused the orientation of the molecular chains. The spot dispersion in Figure 5a_4 was uniform at 500% strain, which indicated that the molecular chains were isotropic. With increasing strain, high-brightness fibrous structures were not observed (Figure 5b).

Using infrared dichroism experiments, it was possible to more fully investigate how silicone rubber oriented itself when it was stretched. The infrared spectrum of MVQ is shown in Figure 5c. 2963 and 2906 cm^{-1} are the asymmetric stretching vibration absorption peak and symmetric stretching vibration absorption peak, respectively [62]. In this paper, the peak at 2906 cm^{-1} is chosen for the orientation analysis of the composite material when it is stretched [63]. Figure 5d depicts the composite's orientation at different strains. The orientation of MVQ, EMVQ15-2.5 and EMVQ15-10 increased gradually with the increased of strain. However, it was shown that the orientation of EMVQ15-5.0 and EMVQ15-7.5 fluctuated. The initial two fluctuations were due to the sliding of molecular chains and the disintegration of topological tangles.

In summary, it was described that the principle of topological entanglement toughened silicone rubber (Figure 6). The steps were as follows: (1) The polycyclic structure was created during the co-blending process of EMVQ and silica. The polycyclic structure of silica was randomly traversed by the silicone rubber matrix's molecular chains, which formed topological entanglement. Many silicas were connected by topological entanglement. (2) When the sample was initially stretched, the molecular chains of the matrix silicone rubber slid on the polycyclic structure. Stress was carried by more molecular chains when the strain was gradually increased. At this time, the molecular chain was entangled with the polycyclic structure and the molecular chain was highly oriented. (3) The path of crack expansion was deflected by the oriented molecular chains in the stretching direction (Figure 3d). (4) The polycyclic structure acts as a fixed pulley to change the direction of the stress. Although the direction of the stress was randomly changed, it might be divided into parallel to the direction of stretching and perpendicular to it. (5) The molecular chains were also highly oriented in the direction perpendicular to the stretching direction. (6) Crack expansion was inhibited by the oriented molecular chains in the direction perpendicular to the stretching direction.

This was why the fibrous structure (high orientation) appeared in Figures 5a_3 and 5a_4. According to the test method and principle of IR color separation, the $(R - 1)/(R + 2)$ of composites with high tear resistance decreased rather than increased at high strain (Figure 5b). In the process, a lot of energy was consumed. The tear resistance of silicone rubber was improved.

4. Conclusions

In summary, silicone rubber with high tear resistance was successfully prepared by adding EMVQ. It is explained how silicone rubber was toughened by EMVQ. The tear strength of the composites increased from 19 to 63 kN/m when 5 phr of EMVQ15, 0.07 phr of a vulcanizing agent, and 40 phr of silica were added. This significantly improved the silicone rubber's tear resistance. The findings of the characterization showed that topological entanglement of

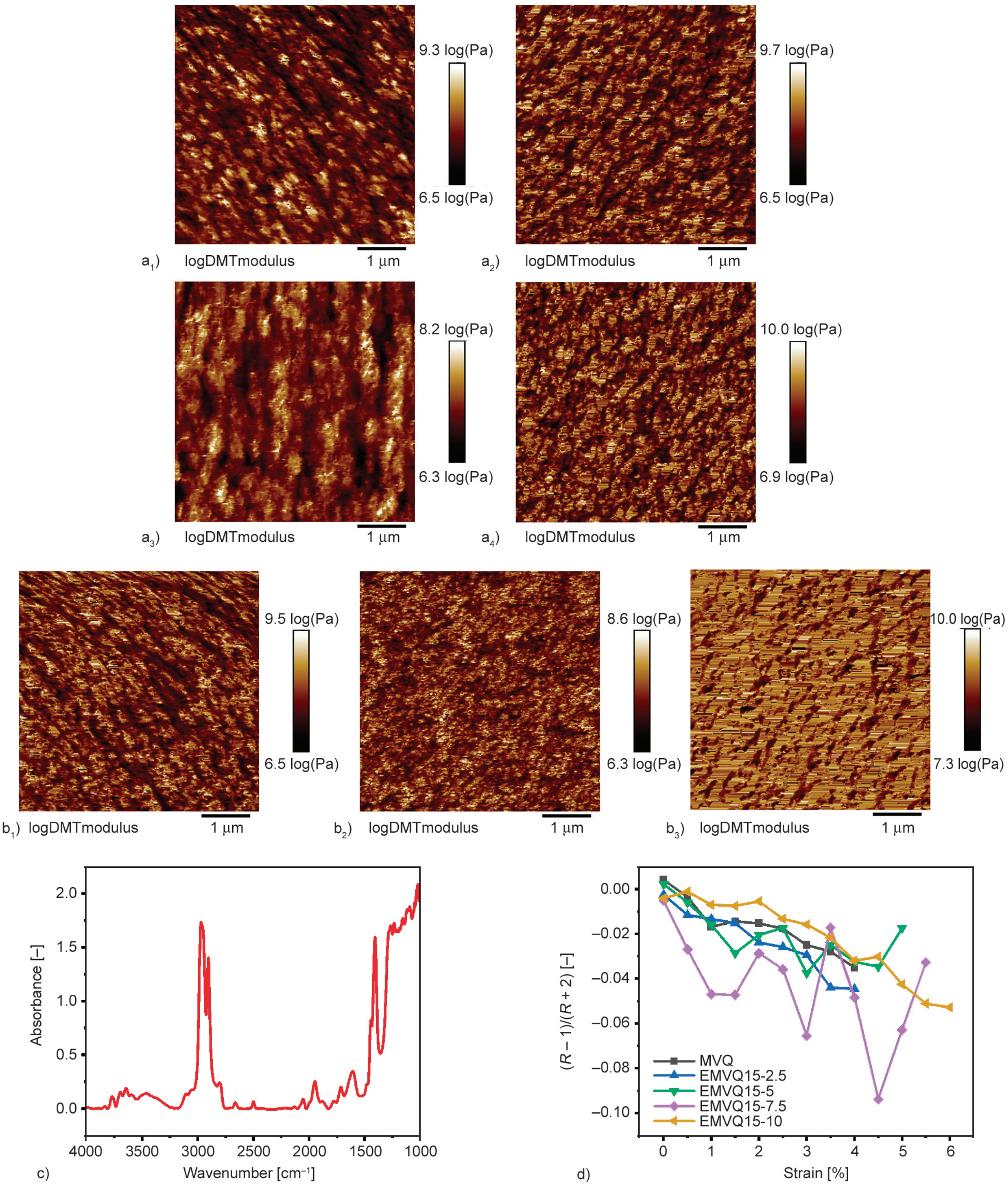

Figure 5. a) The modulus mapping images of EMVQ15-5 with increasing external strain: a_1) 0%, a_2) 100%, a_3) 300%, a_4) 500%; b) the modulus mapping images of MVQ with increasing external strain: b_1) 0%, b_2) 100%, b_3) 300%; c) infrared spectrogram of composite materials; d) $(R-1)/(R+2)$ of the composite at different strains.

polycyclic structure not only concentrated stress during the stretching of the material but also modified the direction of stress transmission and improved the toughness of the material. Silica was dispersed more uniformly in silicone rubber by the addition of EMVQ. The demand for silicone rubber is growing throughout a wide range of industries as they evolve. There are a lot of products, including seals, films, medical silicone tubing, and turbocharger tubes, are made of silicone rubber. However, many silicone rubber products are small parts with complex structures. The products are easily ripped when the heat mold is opened. There are strict requirements for the tear resistance of silicone rubber in harsh

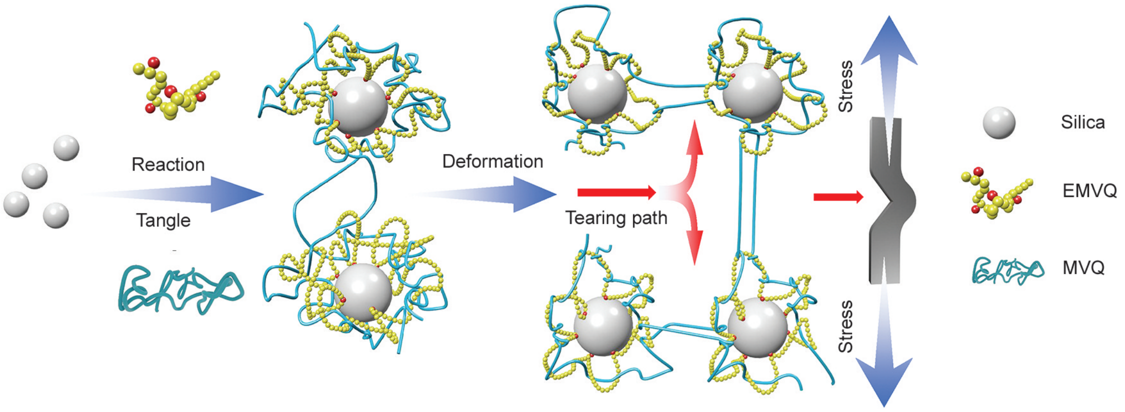

Figure 6. Toughening principle of topological tangles.

situations, such as in the engines of aerospace vehicles. This study can be used to expand the application of silicone rubber. Researchers may come up with innovative ways to toughen other materials as a result of this toughening approach.

References

[1] Zhang Z., Chen P., Nie W., Xu Y., Zhou Y.: Enhanced mechanical, thermal and solvent resistance of silicone rubber reinforced by organosilica nanoparticles modified graphene oxide. Polymer, **203**, 122772 (2020). https://doi.org/10.1016/j.polymer.2020.122772

[2] Tugui C., Cazacu M., Sacarescu L., Bele A., Stiubianu G., Ursu C., Racles C.: Full silicone interpenetrating bi-networks with different organic groups attached to the silicon atoms. Polymer, **77**, 312–322 (2015). https://doi.org/10.1016/j.polymer.2015.09.042

[3] Huang Y., Mu Q., Su Z.: High and low temperature resistance of phenyl silicone rubber. IOP Conference Series: Materials Science and Engineering, **1048**, 012001 (2021). https://doi.org/10.1088/1757-899X/1048/1/012001

[4] Xu R., Luo G., Xia H., He W., Zhao J., Liu B., Tan J., Zhou J., Liu D., Wang Y., Yao Z., Zhan R., Yang S., Wu J.: Novel bilayer wound dressing composed of silicone rubber with particular micropores enhanced wound re-epithelialization and contraction. Biomaterials, **40**, 122221 (2015). https://doi.org/10.1016/j.biomaterials.2014.10.077

[5] Liu P., Li L., Wang L., Huang T., Yao Y., Xu W.: Effects of 2D boron nitride (BN) nanoplates filler on the thermal, electrical, mechanical and dielectric properties of high temperature vulcanized silicone rubber for composite insulators. Journal of Alloys and Compounds, **774**, 396–404 (2018). https://doi.org/10.1016/j.jallcom.2018.10.002

[6] Yang X., Li Q., Li Z., Xu X., Liu H., Shang S., Song Z.: Preparation and characterization of room-temperature-vulcanized silicone rubber using acrylpimaric acid-modified aminopropyltriethoxysilane as a cross-linking agent. ACS Sustainable Chemistry & Engineering, **7**, 4964–4974 (2019). https://doi.org/10.1021/acssuschemeng.8b05597

[7] Eduok U., Faye O., Szpunar J.: Recent developments and applications of protective silicone coatings: A review of PDMS functional materials. Progress in Organic Coatings, **111**, 124–163 (2017). https://doi.org/10.1016/j.porgcoat.2017.05.012

[8] Zhou X., Gong Z., Fan J., Chen Y.: Self-healable, recyclable, mechanically tough transparent polysiloxane elastomers based on dynamic microphase separation for flexible sensor. Polymer, **237**, 124357 (2021). https://doi.org/10.1016/j.polymer.2021.124357

[9] Wolf M., Salieb-Beugelaar G., Hunziker P.: PDMS with designer functionalities – Properties, modifications strategies, and applications. Progress in Polymer Science, **83**, 97–134 (2018). https://doi.org/10.1016/j.progpolymsci.2018.06.001

[10] Chen D., Liu Y., Huang C.: Synergistic effect between poss and fumed silica on thermal stabilities and mechanical properties of room temperature vulcanized (RTV) silicone rubbers. Polymer Degradation and Stability, **97**, 308–315 (2012). https://doi.org/10.1016/j.polymdegradstab.2011.12.016

[11] Kumar V., Mandal T. K., Kumar A., Alam M. N., Parvin N., Joo S. W., Lee D. J., Park S-S.: Multifunctional properties of chemically reduced graphene oxide and silicone rubber composite: Facile synthesis and application as soft composites for piezoelectric energy harvesting. Express Polymer Letters, **16**, 978–995 (2022). https://doi.org/10.3144/expresspolymlett.2022.71

[12] Kumar V., Alam M., Manikkavel A., Song M., Lee D-J., Park S-S.: Silicone rubber composites reinforced by carbon nanofillers and their hybrids for various applications: A review polymers, **13**, 2322 (2021). https://doi.org/10.3390/polym13142322

[13] Zhu Q., Wang Z., Zeng H., Yang T., Wang X.: Effects of graphene on various properties and applications of silicone rubber and silicone resin. Composites Part A: Applied Science and Manufacturing, **142**, 106240 (2021).
https://doi.org/10.1016/j.compositesa.2020.106240

[14] Kumar V., Lee G., Monika, Choi J., Lee D-J.: Studies on composites based on HTV and RTV silicone rubber and carbon nanotubes for sensors and actuators. Polymer, **190**, 122221 (2020).
https://doi.org/10.1016/j.polymer.2020.122221

[15] Zhang Z., Liu Y., Yang K., Chen D., Li S., Li Z.: Reversible thermochromic microencapsulated phase change materials for enhancing functionality of silicone rubber materials. Materials Chemistry and Physics, **290**, 126564 (2022).
https://doi.org/10.1016/j.matchemphys.2022.126564

[16] Shen S., Xin Y., Niu Z., Ma X., Zhang J., Hou X., Ma X.: Phosphazene derivative cross-linked liquid silicone rubber and its mechanical and thermal properties. Polymer Degradation and Stability, **203**, 110086 (2022).
https://doi.org/10.1016/j.polymdegradstab.2022.110086

[17] Liu Z., Huang Y., Yan L., Chen Y., Liang M., Zou H.: Mesophase pitch modified silicone rubber coatings with fence-like ceramic layer structures and excellent ablation resistance performance. Progress in Organic Coatings, **165**, 106773 (2022).
https://doi.org/10.1016/j.porgcoat.2022.106773

[18] Yu F., Lu A., Lu J., Wang Z., Zhang Q., Geng C., Li Z.: Effect of phenyl content, sample thickness and compression on damping performances of silicone rubber: A study by dynamic mechanical analysis and impact damping test. Polymer Testing, **80**, 106101 (2019).
https://doi.org/10.1016/j.polymertesting.2019.106101

[19] Sheng M., Yu J., Gong H., Zhang Y., Wang Y.: Enhancing the thermal stability and mechanical properties of phenyl silicone rubbers by controlling BN addition and phenyl content. Composites Communications, **35**, 101340 (2022).
https://doi.org/10.1016/j.coco.2022.101340

[20] Xu T., Liu H., Song J., Shang S-B., Song Z., Zou K., Yang C.: Synthesis and characterization of maleated rosin-modified fluorosilicone resin and its fluorosilicone rubber. Journal of Applied Polymer Science, **132**, 41888 (2015).
https://doi.org/10.1002/app.41888

[21] Indulekha K., Behera P. K., Rajeev R. S., Gouri C., Ninan K. N.: Polyfluoroalkyl siloxanes with varying trifluoropropyl content: Synthesis, characterization and solvent resistance studies. Journal of Fluorine Chemistry, **200**, 24–32 (2017).
https://doi.org/10.1016/j.jfluchem.2017.05.007

[22] Tan C., Zhou Y., Li J., Zhou H., Xiao Q., Yang X., He S., Li G., Yang Y.: Graphene nanoplatelets/barium titanate hybrid nanoparticles *via* ball milling for enhanced dielectric and mechanical properties of fluorosilicone rubber composites. Ceramics International, in press (2023).
https://doi.org/10.1016/j.ceramint.2022.11.057

[23] Xiong G., Zhang Z., Qi Y.: Effect of the properties of long afterglow phosphors on the antifouling performance of silicone fouling-release coating. Progress in Organic Coatings, **170**, 106965 (2022).
https://doi.org/10.1016/j.porgcoat.2022.106965

[24] Selim M. S., Shenashen M. A., El-Safty S. A., Higazy S. A., Selim M. M., Isago H., Elmarakbi A.: Recent progress in marine foul-release polymeric nanocomposite coatings. Progress in Materials Science, **87**, 1–32 (2017).
https://doi.org/10.1016/j.pmatsci.2017.02.001

[25] Selim M. S., El-Safty S. A., Shenashen M. A., Higazy S. A., Elmarakbi A.: Progress in biomimetic leverages for marine antifouling using nanocomposite coatings. Journal of Materials Chemistry B, **8**, 3701–3732 (2020).
https://doi.org/10.1039/C9TB02119A

[26] Yang X., Li Z., Jiang Z., Wang S., Liu H., Xu X., Wang D., Miao Y., Shang S., Song Z.: Mechanical reinforcement of room-temperature-vulcanized silicone rubber using modified cellulose nanocrystals as cross-linker and nanofiller. Carbohydrate Polymers, **229**, 115509 (2020).
https://doi.org/10.1016/j.carbpol.2019.115509

[27] Song P., Song J., Zhang Y.: Stretchable conductor based on carbon nanotube/carbon black silicone rubber nanocomposites with highly mechanical, electrical properties and strain sensitivity. Composites Part B: Engineering, **191**, 107979 (2020).
https://doi.org/10.1016/j.compositesb.2020.107979

[28] Dong F., Diao S., Ma D., Zhang S., Feng S.: Preparation and characterization of 3-chloropropyl polysiloxane-based heat-curable silicone rubber using polyamidoamine dendrimers as cross-linkers. Reactive and Functional Polymers, **96**, 14–20 (2015).
https://doi.org/10.1016/j.reactfunctpolym.2015.09.005

[29] Li Y-F. S., Zang C-G., Zhang Y-L.: Effect of the structure of hydrogen-containing silicone oil on the properties of silicone rubber. Materials Chemistry and Physics, **248**, 122734 (2020).
https://doi.org/10.1016/j.matchemphys.2020.122734

[30] Chen J., Liu J., Yao Y., Chen S.: Effect of microstructural damage on the mechanical properties of silica nanoparticle-reinforced silicone rubber composites. Engineering Fracture Mechanics, **235**, 107195 (2020).
https://doi.org/10.1016/j.engfracmech.2020.107195

[31] Xue Y., Li X-F., Zhang D-H., Wang H-S., Chen Y., Chen Y-F.: Comparison of ath and SiO_2 fillers filled silicone rubber composites for HTV insulators. Composites Science and Technology, **155**, 137–143 (2018).
https://doi.org/10.1016/j.compscitech.2017.12.006

[32] Tukmachi M. S., Safi I. N., Ali M. M. M.: Evaluation of mechanical properties and cytotoxicity of maxillofacial silicone material after incorporation of zirconia nanopowder. Materials Today: Proceedings, **42**, 2209–2217 (2021).
https://doi.org/10.1016/j.matpr.2020.12.306

[33] Yue Y., Zhang H., Zhang Z., Chen Y.: Polymer–filler interaction of fumed silica filled polydimethylsiloxane investigated by bound rubber. Composites Science and Technology, **86**, 1–8 (2013).
https://doi.org/10.1016/j.compscitech.2013.06.019

[34] Chen J., Liu J., Peng Z., Yao Y., Chen S.: The microscopic mechanism of size effect in silica-particle reinforced silicone rubber composites. Engineering Fracture Mechanics, **255**, 107945 (2021).
https://doi.org/10.1016/j.engfracmech.2021.107945

[35] Liu D., Chen J., Song L., Lu A., Wang Y., Sun G.: Parameterization of silica-filled silicone rubber morphology: A contrast variation sans and tem study. Polymer, **120**, 155–163 (2017).
https://doi.org/10.1016/j.polymer.2017.05.064

[36] Song Y., Yu J., Dai D., Song L., Jiang N.: Effect of silica particles modified by i*n-situ* and *ex-situ* methods on the reinforcement of silicone rubber. Materials & Design, **64**, 687–693 (2014).
https://doi.org/10.1016/j.matdes.2014.08.051

[37] Schaer E., Guizani S., Choplin L.: Model development for the description of silica particles dispersion in silicone polymer. Chemical Engineering Science, **61**, 5664–5677 (2006).
https://doi.org/10.1016/j.ces.2006.04.042

[38] Liu D., Song L., Song H., Chen J., Tian Q., Chen L., Sun L., Lu A., Huang C., Sun G.: Correlation between mechanical properties and microscopic structures of an optimized silica fraction in silicone rubber. Composites Science and Technology, **165**, 373–379 (2018).
https://doi.org/10.1016/j.compscitech.2018.07.024

[39] Xiong Y., Shen S., Kang M., Wang Z., Lu A.: Effect of fluorescence labeling on mechanical properties of silica filled silicone rubber. Polymer, **208**, 122904 (2020).
https://doi.org/10.1016/j.polymer.2020.122904

[40] Fang X., Huang X., Lu Z., Chen L., Chen S.: Synthesis of new superhydrophobic nanosilica and investigation of their performance in reinforcement of polysiloxane. Polymer Composites, **31**, 1628–1636 (2010).
https://doi.org/10.1002/pc.20952

[41] Yan F., Zhang X., Liu F., Li X., Zhang Z.: Adjusting the properties of silicone rubber filled with nanosilica by changing the surface organic groups of nanosilica. Composites Part B-Engineering, **75**, 47–52 (2015).
https://doi.org/10.1016/j.compositesb.2015.01.030

[42] Park J. J., Lee J. Y., Hong Y. G.: Effects of vinylsilane-modified nanosilica particles on electrical and mechanical properties of silicone rubber nanocomposites. Polymer, **197**, 122493 (2020).
https://doi.org/10.1016/j.polymer.2020.122493

[43] Xu Q., Pang M., Zhu L., Zhang Y., Feng S.: Mechanical properties of silicone rubber composed of diverse vinyl content silicone gums blending. Materials & Design, **31**, 4083–4087 (2010).
https://doi.org/10.1016/j.matdes.2010.04.052

[44] Chen W., Zeng X., Li H., Lai X., Fang W., Zeng X.: Influence of nonuniform network on mechanical properties of nano-silica reinforced silicone rubber. Journal of Elastomers and Plastics, **49**, 332–344 (2016).
https://doi.org/10.1177/0095244316661752

[45] Sarath P. S., Samson S. V., Reghunath R., Pandey M. K., Haponiuk J. T., Thomas S., George S. C.: Fabrication of exfoliated graphite reinforced silicone rubber composites – Mechanical, tribological and dielectric properties. Polymer Testing, **89**, 106601 (2020).
https://doi.org/10.1016/j.polymertesting.2020.106601

[46] Cao E., Cui X., Wang K., Li Y., Guo W.: Improving properties of ceramic silicone rubber composites using high vinyl silicone oil. Journal of Applied Polymer Science, **132**, 41864 (2015).
https://doi.org/10.1002/app.41864

[47] Wang Y., Gong Z., Xu C., Chen Y.: Poly (vinylidene fluoride)/fluororubber/silicone rubber thermoplastic vulcanizates prepared through core-shell dynamic vulcanization: Formation of different rubber/plastic interfaces via controlling the core from ‘soft’ to ‘hard’. Materials Chemistry and Physics, **195**, 123–131 (2017).
https://doi.org/10.1016/j.matchemphys.2017.04.016

[48] Dong F., Wang X., Li S., Hao J., Tang X., Kuang R., Wang Y., Feng S.: Applications of α, ω-telechelic polydimethylsiloxane as cross-linkers for preparing high-temperature vulcanized silicone rubber. Polymers for Advanced Technologies, **30**, 932–940 (2019).
https://doi.org/10.1002/pat.4527

[49] Kim J., Zhang G., Shi M., Suo Z.: Fracture, fatigue, and friction of polymers in which entanglements greatly outnumber cross-links. Science, **374**, 212–216 (2021).
https://doi.org/10.1126/science.abg6320

[50] Liu X., Wu J., Qiao K., Liu G., Wang Z., Lu T., Suo Z., Hu J.: Topoarchitected polymer networks expand the space of material properties. Nature Communications, **13**, 1622 (2022).
https://doi.org/10.1038/s41467-022-29245-0

[51] Gao N., Hou G., Liu J., Shen J., Gao Y., Lyulin A., Zhang L.: Tailoring the mechanical properties of polymer nanocomposites *via* interfacial engineering. Physical Chemistry Chemical Physics, **21**, 18714–18726 (2019).
https://doi.org/10.1039/C9CP02948F

[52] Xu T., Jia Z., Luo Y., Jia D., Peng Z.: Interfacial interaction between the epoxidized natural rubber and silica in natural rubber/silica composites. Applied Surface Science, **328**, 306–313 (2015).
https://doi.org/10.1016/j.apsusc.2014.12.029

[53] Kaewsakul W., Noordermeer J. W. M., Sahakaro K., Sengloyluan K., Saramolee P., Dierkes W. K., Blume A.: Natural rubber and epoxidized natural rubber in combination with silica fillers for low rolling resistance tires. in 'Chemistry, manufacture, and application of natural rubber' (eds.: Kohjiya S., Ikeda Y.) Woodhead, Duxford, 247–316 (2021).
https://doi.org/10.1016/B978-0-12-818843-9.00009-6

[54] Birkefeld A. B., Bertermann R., Eckert H., Pfleiderer B.: Liquid- and solid-state high-resolution nmr methods for the investigation of aging processes of silicone breast implants. Biomaterials, **24**, 35–46 (2003).
https://doi.org/10.1016/S0142-9612(02)00241-7

[55] Liang Y., Wang L., Bai Y., Qian H., Xu H., Wang Y.: Study on releasing properties and surface group migration of UV-curable silicone modified polyurethane releasing agent. Progress in Organic Coatings, **164**, 106702 (2022).
https://doi.org/10.1016/j.porgcoat.2021.106702

[56] Shi M., Ao Y., Yu L., Sheng L., Li S., Peng J., Chen H., Huang W., Li J., Zhai M.: Epoxy-poss/silicone rubber nanocomposites with excellent thermal stability and radiation resistance. Chinese Chemical Letters, **33**, 3534–3538 (2022).
https://doi.org/10.1016/j.cclet.2022.03.068

[57] Wang Y., Wu H., Chen Z., Zhou S., Chen Y., Liang M., Zou H.: Silicone-epoxy block hybrid network to achieve high-performance and transparent polydimethylsiloxane materials. Reactive and Functional Polymers, **150**, 104537 (2020).
https://doi.org/10.1016/j.reactfunctpolym.2020.104537

[58] Wang Y., Cao R., Wang M., Liu X., Zhao X., Lu Y., Feng A., Zhang L.: Design and synthesis of phenyl silicone rubber with functional epoxy groups through anionic copolymerization and subsequent epoxidation. Polymer, **186**, 122077 (2020).
https://doi.org/10.1016/j.polymer.2019.122077

[59] Hassanabadi M., Najafi M., Hashemi Motlagh G., Saeedi Garakani S.: Synthesis and characterization of end-functionalized solution polymerized styrene-butadiene rubber and study the impact of silica dispersion improvement on the wear behavior of the composite. Polymer Testing, **85**, 106431 (2020).
https://doi.org/10.1016/j.polymertesting.2020.106431

[60] Li Q., Lin G., Zhang S., Zhang L., Geng C., Borah J.: Enhanced mechanical properties and interfacial interaction of ESBR composites by introducing silica decorated with epoxy functionalized elastomer. Polymer Testing, **112**, 107632 (2022).
https://doi.org/10.1016/j.polymertesting.2022.107632

[61] Wang Z., Liu J., Wu S., Wang W., Zhang L.: Novel percolation phenomena and mechanism of strengthening elastomers by nanofillers. Physical Chemistry Chemical Physics, **12**, 3014–3030 (2010).
https://doi.org/10.1039/b919789c

[62] Cai D., Neyer A., Kuckuk R., Heise H. M.: Raman, mid-infrared, near-infrared and ultraviolet–visible spectroscopy of PDMS silicone rubber for characterization of polymer optical waveguide materials. Journal of Molecular Structure, **976**, 274–281 (2010).
https://doi.org/10.1016/j.molstruc.2010.03.054

[63] Bokobza L., Buffeteau T., Desbat B.: Mid- and near-infrared investigation of molecular orientation in elastomeric networks. Applied Spectroscopy, **54**, 360–365 (2000).
https://doi.org/10.1366/0003702001949636